

Microstructures evolution in MR suspensions governed by Mason number

Sonia Melle^{1,2}, Oscar G. Calderón³, Miguel A. Rubio¹, and Gerald G. Fuller²

¹ Dpto. Física Fundamental, UNED, Senda del Rey 9, Madrid 28040, (Spain).

² Dpt. Chemical Engineering, Stanford University, Stanford, CA 94305-5025, (USA)

³ Dpto. Óptica, UCM, Ciudad Universitaria s/n, Madrid 28040, (Spain)

Introduction

Magnetic fluids exhibit interesting dynamical behavior when subjected to rotating magnetic fields as has been reported in previous studies on magnetic holes [1,2] and magnetic droplets [3,4]. Similar to the behavior of liquid crystals [5,6], these systems show synchronous and non-synchronous regimes depending on the value of the driving frequency. J.C. Bacri et al. [3] found unexpected spiny, starfish shaped magnetic droplets when a high frequency rotating magnetic field was applied. At lower frequencies, O. Sandre et al. [4] found that the magnetic droplets break up to decrease their viscous drag and facilitate tracking the field rotation. Computer simulations of colloidal suspensions subjected to high frequency biaxial fields have been developed by J.E. Martin et al. [7-9]. They predicted the formation of 2D sheet-like structures aligned in the field plane.

In a previous work [10,11], we used scattering dichroism to study the orientation dynamics of low concentrated MR suspensions ($\phi \sim 0.01$) when rotating magnetic fields of moderate frequencies (up to 10 Hz) were applied. In these suspensions, dichroism arises from the formation of optically anisotropic chains upon imposition of the magnetic field and gives information about the number of aggregated particles. With these experiments we simultaneously measured the dichroism ($\Delta n''$) and the orientation angle of the structures. We found that the induced chain-like aggregates rotate synchronously with the field but lag behind with a constant phase angle α . Furthermore, within this synchronous regime, two different behaviors were found below or above a crossover frequency. Below this value, the dichroism remains almost constant while the phase lag increases very rapidly but above the

crossover frequency, the viscous drag overcomes the magnetic force and reduces the dichroism following a power law with an exponent -1.

In this work, scattering dichroism and video microscopy experiments have been combined to study the interplay between magnetic and viscous forces over the crossover frequency separating these two regions. Non-thermal particle dynamics simulations are also reported, showing good agreement with the experiments.

A dimensionless parameter that compares these two forces is the well-known Mason number (ratio of viscous to magnetic forces). This number has been defined with different proportionality factors in literature [12-14]. We define it as follows:

$$\text{Ma} \equiv \frac{12^2 \eta \omega}{\mu_0 \mu_s M^2}, \quad (1)$$

where η is the solvent viscosity, ω is the field rotational frequency, M is the particle magnetization, and μ_0 and μ_s are the vacuum and solvent magnetic permeabilities, respectively.

Experimental Methods

The experiments were performed using suspensions of superparamagnetic micro-spheres loaded with iron oxide grains (see Table 1). Because the techniques we are using need optical transparency, the suspension was sandwiched between two circular quartz windows with diameter ~ 6.5 cm, separated 100 μm along the Z-axis and held in place by a delrin attachment. The sample is surrounded by two orthogonal pairs of coils that generate rotating magnetic fields in the XY plane. The light follows the up-down direction (along the Z-axis).

Scattering dichroism setup

Monochromatic light produced by a He-Ne laser ($\lambda_L=632.8$ nm) is sent through a polarizer oriented at 0° (reference angle of the optical system), a photoelastic modulator (PEM) at 45° and a quarter wave plate at 0° . The PEM produces a time dependent retardation given by $\delta = A \sin(\omega_{PEM}t)$, where A is the amplitude, and $\omega_{PEM} = 50$ kHz is the frequency. The light is then passed through the sample and the transmitted light is detected by a photodiode. The signal from the photodiode is then sent to two phase lock-in amplifiers, one of which extracts the signal component at the frequency of the PEM and the other which extracts the signal component at the second harmonic. The DC component of the light is isolated by passing the transmitted beam through a high pass filter. The three voltages are then digitized and measured using 16-bit analog-to-digital data acquisition device (National Instruments). With this optical train we can simultaneously calculate the dichroism and the orientation angle. A full description of the experimental technique can be found in Refs. [10,15].

Videomicroscopy setup

We illuminated the sample from the top side using a light source with flexible bundle. To amplify the images, we used the *Navitar-12x* zoom system, with which a resolution of $0.34\text{--}4.2$ μm for fields of view around $170\text{--}2100$ μm can be achieved. The images were recorded with a CCD video camera and then digitized on a computer for their subsequent analysis.

Table 1. Characteristics of the magnetic suspensions

| Videomicroscopy | Scattering dichroism |
|---------------------------------|---------------------------------|
| 0 % glycerol | 82.5 % glycerol |
| $\phi = 0.0001$ | $\phi = 0.016$ |
| diameter = 1.24 μm | diameter = 0.87 μm |
| Magnetic content 61 % | Magnetic content 24.8 % |

Results and Discussion

Scattering dichroism experiments

We used scattering dichroism to study the interplay between viscous and magnetic forces on the dynamics of MR suspensions under rotating magnetic fields. As we previously showed [10], two different behaviors for the dichroism and the phase lag are found below or above a crossover frequency. We have studied the dependence of

the crossover frequency on the magnetization by applying magnetic fields with different amplitudes on the same suspension. The dependence of the crossover frequency on the viscosity of the carrier fluid was analyzed applying a constant field on suspensions with different glycerol concentrations. We found that the crossover frequency increases linearly with the square of the magnetization and decreases with the inverse of the viscosity, so the Mason number governs the dynamics. As expected from this result, we obtained a good collapse of the dichroism and the phase lag curves (measured at different magnetic fields and viscosities) with Mason number (see Fig. 1). The change in behavior of the dichroism and the phase lag occurs at a crossover Mason number, $Ma_c \sim 1$, above which the viscous forces dominate and inhibit the aggregation process, being this the mechanism responsible for the decrease of dichroism.

Videomicroscopy experiments

To better understand the dynamics governing MR suspensions under rotating magnetic fields, we performed video microscopy experiments on low volume fraction suspensions ($\phi \sim 0.0001$) for Ma values similar to the ones used on the scattering dichroism experiments presented above.

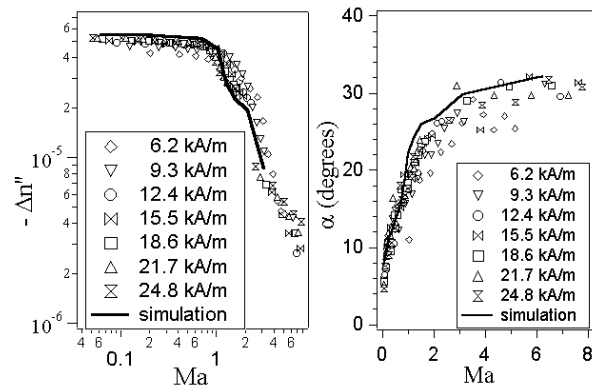


Figure 1. Collapse of dichroism and phase lag with Mason number for different magnetic field strengths

Direct observations show that chains rotate synchronously with the field adjusting their size to decrease their viscous drag (see Fig. 2). The average size of the aggregates decreases with frequency following a power law behavior with an exponent close to -0.5 , the same exponent found in steady shear experiments with constant fields [16]. For $Ma \ll 1$, although the length of the chains decreases with frequency, the number of

aggregated particles (dichroism) remains almost constant supporting the scattering dichroism findings.

However, once the crossover Mason number is surpassed, the viscous forces dominates the magnetic ones and the aggregation process is inhibited increasing the number of isolated particles, i. e. decreasing the dichroism. Furthermore, for $Ma \gg 1$ this magnetic field value is not strong enough for the structures to remain aligned in the field direction and disk-like structures formed by 4-6 particles can be observed (see right image in Fig. 2). As these structures are more isotropic a decrease of dichroism is induced. These structures also rotate with or against the field. Similar structures were found on electrorheological fluids subjected to high frequency rotating fields [17].

For this low field, fragmentation and aggregation processes are observed at low frequencies. As an example, the break up process of a rotating with frequency $f = 0.01$ Hz is shown in Fig. 3. This S shape has been also reported for chains subject to shear in the direction perpendicular to the field [16], and also for magnetic droplets under rotating fields [4].

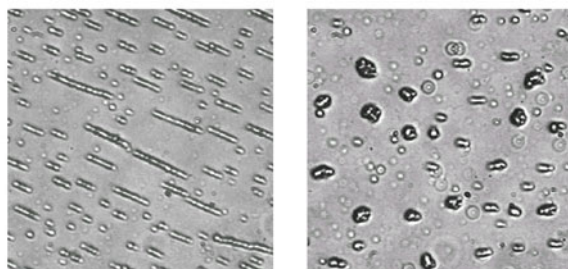


Figure 2. Video-microscopy images recorded after 300s of applying a magnetic field with amplitude $H=1.55$ kA/m for different rotational frequencies. $Ma = 0.0012$ (right). $Ma = 1.2$ (left). Field of view: $43 \times 43 \mu\text{m}$



Figure 3. Detail of the S shape of a chain induced on the same suspensions when a magnetic field of amplitude $H=1.55$ kA/m rotates counter clockwise with $f = 0.01$ Hz. Field of View: $14.4 \times 14.2 \mu\text{m}$

Simulations

In order to interpret the experimental results we developed non-thermal molecular dynamics simulations in 2D. The particles are essentially hard spheres with induced dipolar interactions and Stokes friction against the solvent. The inertial term is neglected because the viscous drag term dominates.

The simulations reveal that the magnetic dipolar interaction induces the formation of chainlike structures that follow the magnetic field rotating with the same frequency in agreement with the experimental findings. In Fig. 4 we plot the particles position in the XY plane for different frequencies (Mason numbers) at an arbitrary time. As demonstrated in this figure, the size of the structures becomes smaller as the rotating frequency increases. This indicates that hydrodynamic friction forces overcome the dipolar magnetic forces and therefore the chains break up to decrease their viscous drag.

The average length of the chains decreases with frequency following a power law with an exponent close to -0.5 , in agreement with the video microscopy results.

The calculated number of aggregated particles and phase lag are shown in Fig. 1 (solid line). Two different regimes appear in agreement with the experimental results.

210 Electrorheology and Magnetorheology

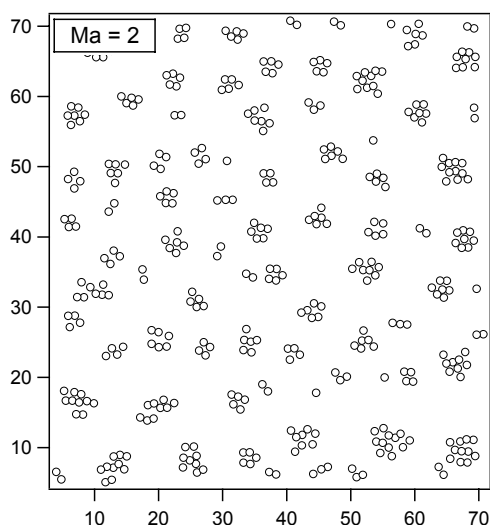
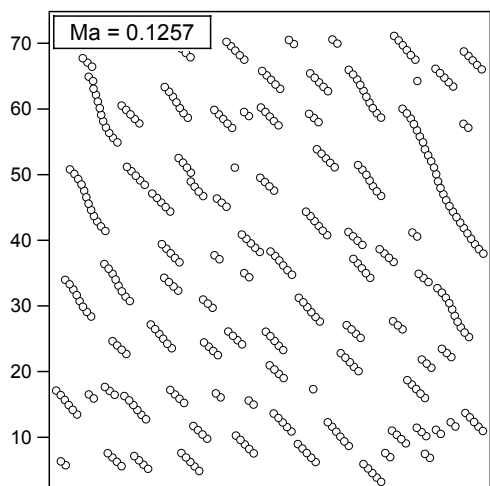


Figure 4. Dimensionless particles positions for different Mason numbers above and below the crossover Mason number at an arbitrary time. Calculations for suspension 82.5% glycerol with volume fraction $\phi=0.016$

References

1. G. Helgesen, P. Pieranski, and A.T. Skjeltorp, Phys. Rev. Lett. 64 (1990) 1425.
2. G. Helgesen, P. Pieranski, and A.T. Skjeltorp, Phys. Rev. A 42 (1990) 7271.

3. J.C. Bacri, A. Cebers, and R. Perzynski, Phys. Rev. Lett. 72 (1994) 2705.
4. Sandre O. et al., Phys. Rev. E 59 (1999) 1736.
5. K.B. Migler and R.B. Meyer, Phys. Rev. E 48 (1993) 1218.
6. C. Zheng and R.B. Meyer, Phys. Rev. E 55 (1997) 2882.
7. J.E. Martin, R.A. Anderson, and C.P. Tigges, J. Chem. Phys. 108 (1998) 7887.
8. J.E. Martin, R.A. Anderson, and C.P. Tigges, J. Chem. Phys. 110 (1999) 4854.
9. J.E. Martin et al., Phys. Rev. E 61 (2000) 2818.
10. S. Melle, G.G. Fuller, and M.A. Rubio, Phys. Rev. E 61 (2000) 4111.
11. S. Melle et al., J. Colloid Interface Sci. 247 (2002) 200.
12. Mason number was first introduced in literature for ER fluids under steady shear. See A.P. Gast, and C.F. Zukoski, Adv. Colloid Interface Sci 30 (1989) 153
13. O. Volkova, S. Cutillas, and G. Bossis, Phys. Rev. Lett. 82 (1999) 233.
14. J.E. Martin, Phys. Rev. E 63 (2001) 011406
15. G.G. Fuller, Optical rheometry of complex fluids, Oxford University Press (1995).
16. J.E. Martin et al., J. Chem. Phys. 104 (1996) 4814.
17. T.C. Halsey, R.A. Anderson, and J.E. Martin, Int. J. Modern Phys. B 10 (1996) 3019.

Contact Address:

Sonia Melle (smelle@fisfun.uned.es)
 Dpto. Física Fundamental, Facultad de Ciencias. UNED, c./
 Senda del Rey 9, 28040 Madrid (Spain)
 Telf.: +34 913987142; Fax: +34 913986697;